down in helium and argon," *J. Phys. D.: Appl. Phys.*, vol. 4, pp. 225–235, 1971.
[10] B. F. Mulchenko and C. P. Raizer, "Laser breakdown of mixtures of neon with argon and the role of photoionization of excited atoms," *Sov. Phys.–JETP*, vol. 33, pp. 349–353, Aug. 1971.
[11] N. S. Kopeika, A. P. Kushelevsky, and G. Eytan, "Photoionization of excited atoms in dc gas discharges by low intensity light and its application to gas breakdown study with highly intense lasers," to be published.
[12] N. S. Kopeika, J. Rosenbaum, and R. Kastner, "Abnormal glow discharge detection of visible radiation," *Appl. Opt.*, vol. 15, pp. 1610–1615, June 1976.
[13] N. S. Kopeika and J. Rosenbaum, "Subnormal glow discharge detection of optical and microwave radiation," *IEEE Trans. Plasma Sci.*, vol. PS-4, pp. 51–61, Mar. 1976.
[14] R. B. Green, R. A. Keller, G. G. Luther, P. K. Schenk, and J. C. Travis, "Galvanic detection of optical absorptions in a gas discharge," *Appl. Phys. Lett.*, vol. 19, pp. 72–74, Dec. 1, 1976.
[15] —, "Use of an opto-galvanic effect to frequency-lock a continuous wave dye laser," *IEEE J. Quantum Electron.* (corresp.), vol. QE-13, pp. 63–64, Feb. 1977.
[16] N. S. Kopeika and G. Eytan, "Photoionization of excited atoms in gas-filled photodiodes: Improved detectivity with microsecond order risetimes," *IEEE Trans. Plasma Sci.*, to be published.
[17] G. Eytan, N. S. Kopeika, R. Gellman, and A. P. Kushelevsky, "A sensitive ultraviolet radiation detector based on photoionization of excited atoms," *Opt. Quantum Electron.*, vol. 9, pp. 354–356, July 1977.
[18] N. S. Kopeika, R. Gellman, and A. P. Kushelevsky, "Improved detection of ultraviolet radiation with gas-filled phototubes through photoionization of excited atoms," *Appl. Opt.*, vol. 16, pp. 2470–2478, Sept. 1977.
[19] J. M. W. Milatz and L. S. Ornstein, "The electronic excitation function of the metastable S_5 level of neon," *Physica* (Utrecht), vol. 2, pp. 355–367, Feb. 1935.
[20] N. G. Basov, V. A. Danilychev, O. M. Kerimov, and A. S. Podsosonnyi, "Population inversion in the active medium of an electroionization CO_2 laser at a working-mixture pressure up to 20 atmospheres," *JETP Lett.*, vol. 17, pp. 102–104, 1973.
[21] A. Von Engel, *Ionized Gases*. Oxford: Clarendon, 1965, p. 73.
[22] W. J. Price, *Nuclear Radiation Detection*. New York: McGraw-Hill, 1964, p. 81.
[23] J. A. Bearden, "Radioactive contamination of ionization materials," *Rev. Sci. Instr.*, vol. 4, pp. 271–275, May 1933.
[24] V. K. Zworykin and E. G. Ramberg, *Photoelectricity and Its Application*. New York: Wiley, 1949, pp. 120–135.
[25] H. J. J. Seguin, D. McKen, and J. Tulip, "Photoabsorption and ionization cross sections in a seeded CO_2 laser mixture," *Appl. Opt.*, vol. 16, pp. 77–82, Jan. 1977.
[26] M. C. Richardson, K. Leopold, and A. J. Alcock, "Large aperture CO_2 laser discharges," *IEEE J. Quantum Electron.*, vol. QE-9, pp. 934–939, Sept. 1973.
[27] O. P. Judd, "An efficient electrical CO_2 laser using preionization by ultraviolet radiation," *Appl. Phys. Lett.*, vol. 22, pp. 95–96, Feb. 1, 1973.
[28] L. E. Kline, L. J. Denes, and M. J. Pechersky, "Arc suppression in CO_2 laser discharges," *Appl. Phys. Lett.*, vol. 29, pp. 574–576, Nov. 1, 1976.
[29] Ch. Homann and H. Hubner, "Slow discharge in superatmospheric CO_2-N_2-He gas mixtures in a Lamberton-Pearson device," *Phys. Lett.*, vol. 55A, pp. 287–288, Dec. 29, 1975.
[30] H. Hubner and C. Homann, "Characteristics of CO_2 TE-amplifiers with different UV preionization at superatmospheric pressure with doping additives," *Appl. Phys.*, vol. 12, pp. 211–212, 1977.
[31] P. Weiss, "Attenuation of 10.6 μm beams by electrically initiated laser driven plasmas," *Appl. Phys. Lett.*, vol. 30, pp. 261–263, Mar. 15, 1977.

Numerical Analysis of Laser Induced Inelastic Collisions

STEPHEN E. HARRIS, FELLOW, IEEE, AND JONATHAN C. WHITE

Abstract—**This paper studies the dynamics of (dipole-dipole) laser induced collision processes. Coupled equations are numerically integrated, first over time, and then over impact parameter. Transition probability and collision cross section are given as a function of the detuning from the $R = \infty$ frequency of the separated atoms, and of the incident laser power density. Numerical results are compared with approximate formulae for collision cross section at line center and in the wing.**

INTRODUCTION

IF the energy defect ΔE between the initial and final states of two colliding atoms is large with respect to kT, then the cross section for inelastic collision will be quite small. This paper considers processes where one or more photons are utilized to satisfy this energy defect.

If the photon (or photons) is supplied by an incident laser, the process may be considered as a "switched" collision. Without the laser radiation present, the collision cross section is very small (perhaps 10^{-20} cm^2). With the laser beam present, the collision cross section rises, with a rise time equal to that of the laser, to a value as large as 10^{-12} cm^2.

Alternately, a photon may be emitted (spontaneously or stimulated) as the two atoms collide. Such radiative collisions allow the construction of lasers with a center frequency equal to the difference of the energy levels of two different species.

Following theoretical predictions by Gudzenko and Yakovlenko [1], and somewhat later by Harris and Lidow [2], the first experimental observations of this process have recently been reported [3], [4]. The experiments of [3]

Manuscript received August 1, 1977; revised September 2, 1977. This work was jointly supported by the Air Force Rome Air Development Center under Contract F19628-77-C-0072 and the Office of Naval Research under Contract N00014-75-C-0576.

The authors are with the Edward L. Ginzton Laboratory, Stanford University, Stanford, CA 94305.

involved storage in the $Sr(5p^1P^0)$ resonance level and transfer to selected states of Ca. Those of [4] involved storage in Eu and transfer to the $5p^2\ ^1D_2$ level of Sr. Both experiments confirmed the key prediction, that for dipole-dipole collisions, the collision cross section should maximize when the incident laser is tuned to the interatomic frequency of the infinitely separated atoms.

Fig. 1 shows an energy-level diagram for a prototype collision system. We assume storage in level $|a_2\rangle$ of atom A. As atoms A and B approach each other, they undergo what may be termed a virtual collision, in which atom A is de-excited and atom B excited. The process is completed by absorption of the photon of energy $\hbar\omega$. The virtual collisional excitation occurs in the same sense as does that caused by the first photon of a two-photon absorption; or by the incident photon which results in Rayleigh scattering.

A goal of this paper is to study the dependence of collision cross section on the detuning $\delta\omega$ (Fig. 1) from the energy difference of the energy levels $|b_3\rangle$ and $|a_2\rangle$ of the infinitely separated atoms. This is accomplished by numerically integrating the pertinent coupled equations over time, and then over impact parameter. Results are given for both the low and high electromagnetic field cases, and in the low field case are compared with approximate formulae.

Other studies of the lineshape of laser induced collision processes have been given by Lisitsa and Yakovlenko [5], Gallagher and Holstein [6], and by Payne *et al.* [7]. Different aspects of the laser collision problem have been treated by many authors [8]-[18].

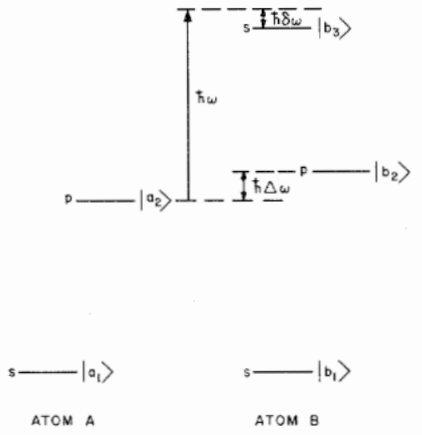

Fig. 1. Prototype system for a laser-induced collision. Energy is stored in the $|a_2\rangle$ state of atom A and transferred to the $|b_3\rangle$ state of atom B by means of laser radiation at frequency ω. The detuning of ω from the energy difference of the energies of levels $|b_3\rangle$ and $|a_2\rangle$ of the infinitely separated atoms is denoted by $\delta\omega$.

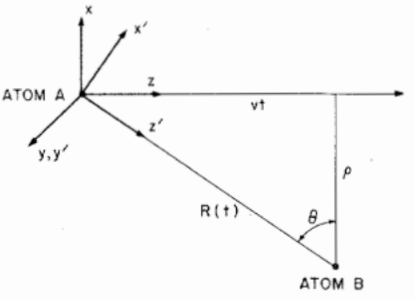

Fig. 2. Coordinate system for analysis. Atom A moves with velocity V along the z axis. The unprimed coordinate system is fixed in space, while in the primed system the z' axis points along the internuclear axis and therefore rotates during the course of the collision.

Equation Development

We start by expanding the wave function in a basis set of product eigenfunctions of the infinitely separated atoms:

$$\psi = \sum_{n=1}^{3} c_n(t)\,|\mu_n\rangle \exp(-jE_n t/\hbar). \tag{1}$$

We retain only the three product states $|\mu_1\rangle = |a_2\rangle|b_1\rangle$, $|\mu_2\rangle = |a_1\rangle|b_2\rangle$, and $|\mu_3\rangle = |a_1\rangle|b_3\rangle$. The E_n in (1) are therefore the sum energies of the pertinent states of the infinitely separated atoms, and are not functions of position or time. For example, E_1 is the sum of the energies of states $|a_2\rangle$ and $|b_1\rangle$.

We assume the coordinate system shown in Fig. 2, where atom B is fixed and atom A moves in a straight line with velocity V along the z axis. The relative distance of the two atoms, as a function of time, is $R^2(t) = \rho^2 + V^2t^2$, where the quantity ρ is termed as the impact parameter. We assume that the incident laser beam has frequency ω and is polarized along the y axis, i.e., $E(t) = E\hat{a}_y \cos \omega t$. The classical interaction Hamiltonian may then be written

$$H(t) = -ey_A E \cos\omega t - ey_B E \cos\omega t + \frac{e^2}{R^3(t)}(x'_A x'_B + y'_A y'_B - 2z'_A z'_B). \tag{2a}$$

The coordinates x_A, x_B, x'_A, x'_B, etc., denote the position of each electron with respect to its nucleus. The unprimed system is fixed in space (Fig. 2), while in the primed system, the z' axis points along the interatomic axis, and therefore rotates with respect to the unprimed system during the collision, i.e.,

$$\begin{aligned} x' &= x\sin\theta + z\cos\theta \\ z' &= z\sin\theta - x\cos\theta \\ y' &= y \end{aligned} \tag{2b}$$

where $\cos\theta = \rho/R(t)$. During the course of the collision θ varies from $-\pi/2$ to $\pi/2$.

We now substitute (1) into Schrödinger's equation, and take matrix elements of (2). In doing so, we make what is termed as the fixed atom approximation. In a classical sense, this means that we assume that the orientation of the dipole moment of the p state atom is random with regard to the s state atom; and that this orientation remains unchanged during the course of a collision. Quantum mechanically (Appendix), this is carried out by assuming that occupation of each of the three degenerate m states is equally probable, and separately computing and averaging their contributions.

We thereby obtain the coupled equations

$$\frac{\partial c_1}{\partial t} = \frac{j}{\hbar}\left(\frac{2}{\sqrt{3}}\right)\frac{\mu^{A1}\mu^{B1}}{R^3(t)}c_2 \exp(-j\Delta\omega t) \tag{3a}$$

$$\frac{\partial c_2}{\partial t} = \frac{j}{\hbar}\left(\frac{2}{\sqrt{3}}\right)\frac{(\mu^{A1}\mu^{B1})^*}{R^3(t)} c_1 \exp(+j\Delta\omega t) + \frac{j}{\hbar}\frac{\mu^{B2}E}{2} c_3 \exp[+j(\Delta\omega+\delta\omega)t] \quad (3b)$$

$$\frac{\partial c_3}{\partial t} = \frac{j}{\hbar}\frac{(\mu^{B2}E)^*}{2} c_2 \exp[-j(\Delta\omega+\delta\omega)t]. \quad (3c)$$

The matrix elements in these equations are now those which are seen by linearly polarized light, i.e.: $\mu^{A1} \equiv \langle a_2 | z_A | a_1 \rangle$, $\mu^{B1} \equiv \langle b_1 | z_B | b_2 \rangle$, and $\mu^{B2} \equiv \langle b_2 | y_B | b_3 \rangle$. The quantities $\hbar\Delta\omega$ and $\hbar\delta\omega$ are the separation of the initial $|\mu_1\rangle = (|a_2\rangle|b_1\rangle)$ and intermediate $|\mu_2\rangle = (|a_1\rangle|b_2\rangle)$ product states and the detuning from the final state (Fig. 1).

If $\Delta\omega$ is large compared to the relative rate of change of c_1, c_3, and $1/R^3(t)$, then (3b) may be integrated and substituted into (3a) and (3c). We obtain

$$\frac{\partial c_1}{\partial t} = \frac{j}{\hbar}\left[\left(\frac{4}{3}\right)\frac{1}{\hbar\Delta\omega}\frac{|\mu^{A1}\mu^{B1}|^2}{R^6(t)}\right]c_1 + \frac{j}{\hbar}\left[\frac{2}{\sqrt{3}}\frac{\mu^{B2}E}{2\hbar\Delta\omega}\frac{\mu^{A1}\mu^{B1}}{R^3(t)}\right]c_3 \exp(+j\delta\omega t) \quad (4a)$$

$$\frac{\partial c_3}{\partial t} = \frac{j}{\hbar}\left(\frac{1}{\hbar\Delta\omega}\left|\frac{\mu^{B2}E}{2}\right|^2\right)c_3 + \frac{j}{\hbar}\left[\frac{2}{\sqrt{3}}\left(\frac{\mu^{B2}E}{2\hbar\Delta\omega}\right)^*\frac{(\mu^{A1}\mu^{B1})^*}{R^3(t)}\right]c_1 \exp(-j\delta\omega t). \quad (4b)$$

The first term in (4a) is recognized as the van der Waals shift of the product state $|\mu_1\rangle$, caused by the presence of $|\mu_2\rangle$; while the first term in (4b) is the ac Stark shift of the product state $|\mu_3\rangle$.

We now define the quantities

$$C_3 \equiv \frac{2}{\sqrt{3}}\frac{\mu^{A1}\mu^{B1}\mu^{B2}}{2\hbar\Delta\omega}\mathrm{E} \quad (5a)$$

$$C_6 \equiv \frac{4}{3}\frac{|\mu^{A1}\mu^{B1}|^2}{\hbar\Delta\omega} \quad (5b)$$

$$B \equiv \frac{|\mu^{B2}|^2}{4\hbar\Delta\omega}|E|^2 \quad (5c)$$

and change variables according to

$$a_1 = c_1 \exp\left[-\frac{j}{\hbar}\int_{-\infty}^{t}\frac{C_6}{R^6(t)}dt\right]$$

$$a_3 = c_3 \exp\left[-\frac{j}{\hbar}\int_{-\infty}^{t} B\,dt\right]. \quad (6)$$

Equations (4a) and (4b) then become

$$\frac{\partial a_1}{\partial t} = \frac{j}{\hbar}\frac{C_3}{R^3(t)}a_3 \exp\left\{+\frac{j}{\hbar}\int_{-\infty}^{t}\left[\frac{-C_6}{R^6(t)}+B+\delta\omega\right]\right\}dt \quad (7a)$$

$$\frac{\partial a_3}{\partial t} = \frac{j}{\hbar}\frac{C_3^*}{R^3(t)}a_1 \exp\left\{-\frac{j}{\hbar}\int_{-\infty}^{t}\left[\frac{-C_6}{R^6(t)}+B+\delta\omega\right]\right\}dt. \quad (7b)$$

Note that both C_3 and B depend on the strength of the applied laser field.

The problem has thus been reduced to a two-state problem having an effective interaction Hamiltonian and energy levels, both of which are functions of the internuclear spacing R. By varying the strength of the electromagnetic field, the magnitude of the interaction Hamiltonian is varied. By varying the frequency of the electromagnetic field, in effect, a curve crossing is created at arbitrary R.

To the extent that no other atomic states are pertinent to the problem, then the only approximation which has been made in (7) is that $\Delta\omega$ be large compared to the inverse time of a collision and to the rate of change of a_1 and a_3. To the extent that other states are pertinent and shift the energies of either $|\mu_1\rangle$ or $|\mu_3\rangle$, their contribution may be taken into account by using a corrected relative C_6. Equations (7a) and (7b) were first given by Gudzenko and Yakovlenko [1] and were arrived at by first using stationary perturbation theory at fixed R, and then applying the electromagnetic field. The approximation with regard to $\Delta\omega$ is thus implicit, but is the same as that which we have made here. Fig. 3 shows the laser collision process in the two-state, or quasi-molecular viewpoint.

The calculated values of the quantities that appear in (7) for the recent experiment [3]

$$\mathrm{Sr}(5p^1P^0) + \mathrm{Ca}(4s^2\ ^1S) + \hbar\omega(4977\ \text{Å}) = \mathrm{Sr}(5s^2\ ^1S) + \mathrm{Ca}(4p^2\ ^1S) \quad (8)$$

are $C_6/\hbar = -4.2 \times 10^7$ cm^{-1} Å^6; that is, the relative energy shift is -42 cm^{-1} when the atoms are separated by a distance of 10 Å.[1] The Stark shift quantity $B/\hbar$ may be expressed as $B/\hbar = 5.5 \times 10^{-10}$ cm^{-1} (P/A) (W/cm^2); thus at an applied power density of P/A $= 10^{10}$ W/cm^2, $B/\hbar = 5.5$ cm^{-1}. The interaction constant $C_3/\hbar = 1.6 \times 10^{-1}$ cm^{-1} Å^3 (P/A)$^{1/2}$, with P/A again in units of W/cm^2.

Collision Transition Probability

The procedure of the numerical analysis is to assume a linear trajectory

$$R(t) = (\rho^2 + V^2t^2)^{1/2} \quad (9)$$

and, subject to the boundary condition $|a_1(t=-\infty)|^2 = 1$ and $|a_3(t=-\infty)|^2 = 0$, to use a fourth-order Runge-Kutta algorithm to integrate (7) from $t = -\infty$ to $t = +\infty$. The probability of inelastic collision for a particular ρ and V is $|a_3(\rho, V, t=\infty)|^2$. The velocity averaged cross section is then

[1] The total C_6 is that of (5b) which gives the shift of $|\mu_1\rangle$ [$C_{6(1)}/\hbar = 4.9 \times 10^7$ cm^{-1} Å^6] minus a contribution for the shift of $|\mu_3\rangle$. This latter contribution [$C_{6(2)}/\hbar = 9.1 \times 10^7$ cm^{-1} Å^6] arises predominantly from the interaction with the Sr($6p^1P^0$) and Sr($5p^1P^0$) levels. Thus $C_6 = C_{6(1)} - C_{6(2)}$ is negative.

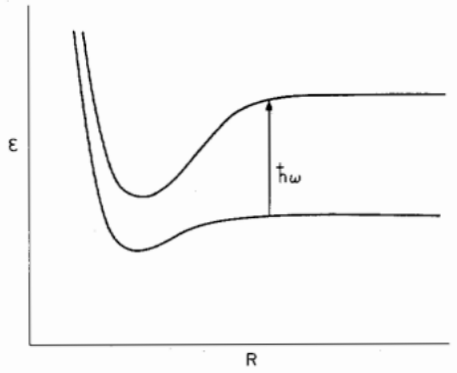

Fig. 3. Laser collision process in the quasi-molecular viewpoint. In the quasi-molecular viewpoint, the energies of the initial and final states depend on the internuclear separation R, and the collision is viewed as a photon-induced transition.

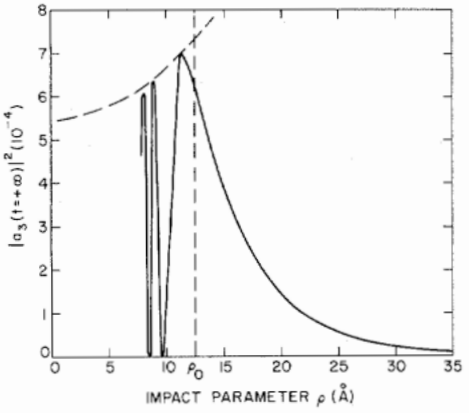

Fig. 4. Collision transition probability as a function of impact parameter ρ for the Sr–Ca system of (8). The laser is assumed to be tuned to line center ($\delta\omega = 0$), and to have a power density of P/A = 5×10^5 W/cm^2. Dotted line shows the position of the relative Weisskopf radius ρ_0.

$$\sigma_c = \int_0^\infty \int_0^\infty |a_3(\rho, V, t=\infty)|^2 f(V)(2\pi\rho)\, d\rho\, dV \qquad (10)$$

where

$$f(V) = \frac{4}{\sqrt{\pi}} \left(\frac{\mu}{2kT}\right)^{3/2} \frac{1}{\overline{V}}\, V^2 \exp - \left(\frac{\mu V^2}{2kT}\right)$$

and the average velocity $\overline{V} = (8kT/\pi\mu)^{1/2}$, where μ is the reduced mass.

Fig. 4 shows the collision transition probability $|a_3(t=\infty)|^2$ as a function of the impact parameter ρ for the laser tuned to exactly the frequency of the energy defect ($\delta\omega = 0$). The transition probability rises as $1/\rho^4$ and reaches a maximum in the vicinity of the relative Weisskopf radius ρ_0, defined as

$$\frac{1}{\hbar}\int_{-\infty}^{+\infty} \frac{|C_6|}{R^6(t)}\, dt = \frac{3\pi}{8}\, \frac{1}{\hbar}\, \frac{|C_6|}{\overline{V}\rho_0^5} = \pi. \qquad (11)$$

For impact parameters less than ρ_0, the transition probability oscillates with decreasing ρ. For the Sr–Ca system discussed above, $C_6 = -4.2 \times 10^7$ cm^{-1} Å^6, $V = 9.6 \times 10^4$ cm/s, and $\rho_0 = 12.5$ Å.

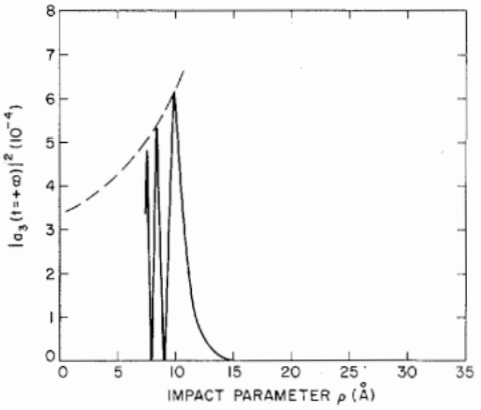

Fig. 5. Collision transition probability as a function of impact parameter ρ, with the laser detuned by -20 cm^{-1}. The other conditions are the same as those of Fig. 4.

It is important to note that about 70 percent of the contribution to the cross section (10) occurs for impact parameters greater than ρ_0. This long-range nature of the interaction allows us to make computations without knowing the interatomic potentials at small R; for example, spin-spin interaction need not be considered.

Fig. 5 shows the collision transition probability as a function of ρ for a detuning from line center of $\delta\omega = -20$ cm^{-1}. This detuning has a sign such that there is an effective curve crossing at some R_x, i.e., at some R_x the argument of the exponent in (7) equals zero at t such that $R(t) = R_x$. As per the Landau-Zener theory of curve crossing collisions, the transition probability is only large for $\rho \leqslant R_x$. At a given impact parameter $a_3(t)$ accumulates during each of the two times that the crossing distance is neared. The oscillation of $|a_3(t=+\infty)|^2$ results from the adding and subtracting of the phased contributions at each of the two crossings.

Note that in the detuned case that significantly more of the contribution to the total collision cross section occurs at small impact parameter than in the on-line-center case, and thus knowledge of the close-in interaction potential is of correspondingly more importance. For the Sr–Ca example $R_x = (C_6/\hbar\delta\omega)^{1/6} = 11.3$ Å, for $\delta\omega = -20$ cm^{-1}

Collision Cross Section and Lineshape

The velocity-averaged collision cross section is obtained by numerically integrating the transition probability, as per (10). The on-line-center ($\delta\omega = 0$), thermal velocity ($T = 300$ K), collision cross section, as a function of laser power density, is shown in Fig. 6 for the Sr–Ca example of (8).

The collision cross section rises linearly with power density to a value of about 10^{-13} cm^2 at P/A = 10^9 W/cm^2, and then begins to saturate. The power density at which the saturated or "strong field" regime begins is approximately that at which the transition probability is equal to unity at an impact parameter equal to ρ_0. In Fig. 6 we have taken the Stark shift constant $B = 0$, thus assuming that the calculated Stark shift

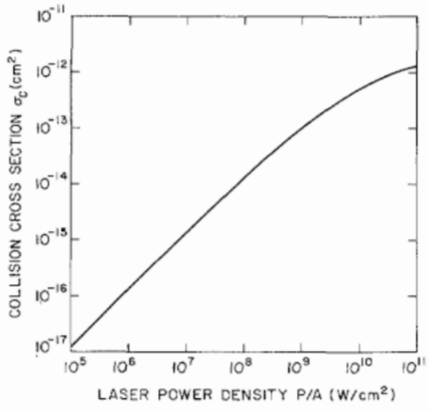

Fig. 6. Collision cross section versus laser power density. Incident laser is assumed tuned to line center. Constants used are those of the Sr–Ca example of (8).

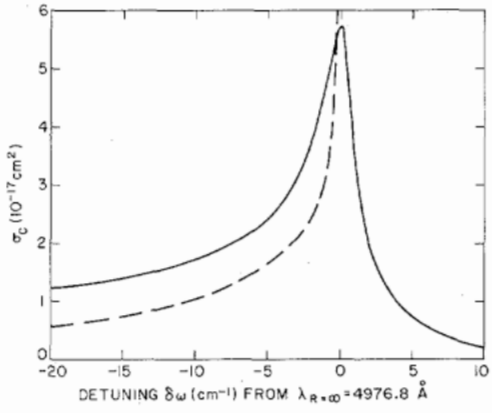

Fig. 7. Collision cross section versus detuning from line center. Parameters are those of the Sr–Ca experiment and the assumed laser power density is 5×10^5 W/cm^2. Dotted line shows the approximate collision cross section as given by (14).

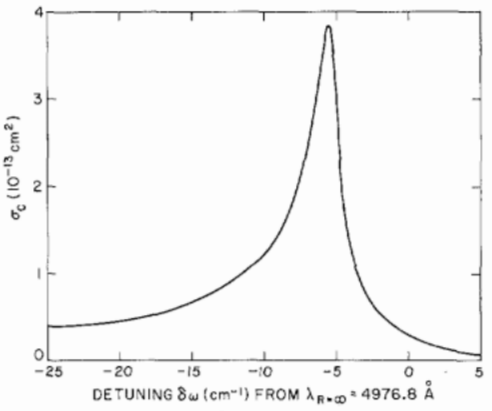

Fig. 8. Cross section versus detuning at high field strength (P/A = 10^{10} W/cm^2). Ratio of peak to wing cross section is greater than that at lower laser power density.

can be tracked. (For the Sr–Ca example, the Stark shift is calculated as 0.5 cm^{-1} at P/A = 10^9 W/cm^2, and varies linearly with power density.)

The calculated collision cross section as a function of the detuning $\delta\omega$ from the $R = \infty$ frequency is shown in Fig. 7. The parameters are those of the Sr–Ca experiment, and the assumed laser power density is 5×10^5 W/cm^2. The cross section maximizes at the $R = \infty$ frequency. On the blue side where there is no effective curve crossing, the falloff is quite abrupt. The finite cross section on the blue side results from transitions caused by the relative motion of the atoms, according to Massey's adiabatic criteria. On the red side, the falloff is much more gradual and corresponds to the Landau–Zener or curve crossing regime of collision theory. Collision cross sections (as a function of detuning) of the form of Fig. 7 have also been calculated by Gallagher and Holstein [6], and Payne *et al.* [7].

Fig. 8 shows σ_c as a function of the detuning $\delta\omega$ at a much higher field strength (P/A = 10^{10} W/cm^2). A significant Stark shift is now present; and, of more importance, the ratio of the peak cross section to that of the wing cross section is increased by about a factor of 2. This line narrowing in the high field limit was predicted by Lisitsa and Yakovlenko [5] and occurs as a result of the $1/R^3$ interaction energy which is linear in the applied electric field strength dominating over the $1/R^6$ energy.

Approximate Formulae

We now give approximate formulae for the on-line-center and wing cross sections. The on-line-center formula is obtained by neglecting depletion of the ground state [taking $a_1(t) = 1$], neglecting the exponential portion of (7b), assuming that the velocity of all atoms equals $\bar{V}$, and integrating (10) from ρ_0 to ∞. We thereby assume that all collisions with impact parameter $\rho > \rho_0$ experience no dephasing, while all collisions with $\rho < \rho_0$ make no contribution to σ_c. This yields

$$\sigma_c = 4\left(\frac{8}{3}\right)^{2/5} \pi\hbar^{-8/5}\, \bar{V}^{-8/5}\, |C_3|^2\, |C_6|^{-2/5} \tag{12}$$

where C_3 and C_6 are defined in (5). For constants of the Sr–Ca example, (12) yields $\sigma_c = 8.4 \times 10^{-23}$ (P/A) cm^2, with P/A in W/cm^2. This value is a factor of 1.4 smaller than that obtained numerically (Fig. 6).

An approximate formula for application in the wing is obtained by assuming that at each of the two curve crossings a cumulative interaction occurs for a time Δt such that

$$\frac{1}{\hbar}\int_{-\Delta t/2}^{+\Delta t/2} \left[\frac{\partial}{\partial R}\left(\frac{|C_6|}{R^6}\right)\right]_{R=R_x} \bar{V}t'\, dt' = \pi \tag{13}$$

or

$$\Delta t = \left(\frac{\pi\hbar R_x^7}{3\bar{V}\,|C_6|}\right)^{1/2}.$$

This leads to

$$\sigma_c = \frac{2}{3}\frac{\pi^2}{\hbar\bar{V}}\frac{|C_3|^2}{|C_6|}R_x^3 \tag{14}$$

where the curve crossing distance $R_x = (C_6/\hbar\delta\omega)^{1/6}$. For the previous constants and $\delta\omega = -20$ cm^{-1}, we have $R_x = 11.3$ Å, $\Delta t = 5.7 \times 10^{-13}$ s, and $\sigma_c = 1.2 \times 10^{-23}$ (P/A) cm^2. This is a factor of 2 smaller than that obtained numerically. σ_c from (14) is shown as the dotted line in Fig. 7. Equation (14) thus gives the correct asymptotic dependence and remains

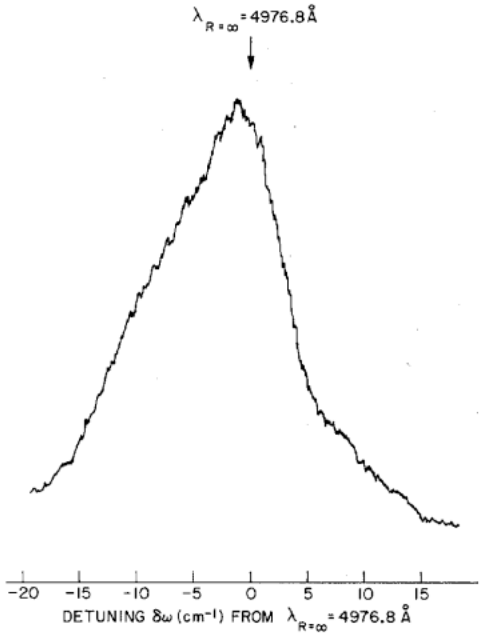

Fig. 9. Experimental lineshape for the Sr–Ca experiment of (8) and [3]. Energy was stored in the Sr($5p^1P^0$) level and transferred to the Ca($4p^2\ ^1S$) level. Energy difference of the initial and final states of the infinitely separated atoms is $\lambda_{R=\infty}$ = 4976.8 Å.

valid until R_x becomes sufficiently large that Δt of (13) begins to approach the impact time $\pi\rho_0/\bar{V}$.

Comparison with Experiment

Fig. 9 shows the experimentally obtained lineshape for the Sr–Ca process of [3] and (8). The lineshape includes the contribution of the ~2 cm^{-1} linewidth of the 4977 Å laser.

To within experimental accuracy, both the measured and calculated (Fig. 7) lineshapes peak at the $R = \infty$ frequency of the separated atoms. And, as expected, they both skew toward the red. The experimental curve is broader than expected and falls off too rapidly in the red wing. Numerical trials indicate that this more rapid fall-off is probably not due to an incorrect calculation of C_6. The discrepancy may be due to the close-in interaction potentials differing significantly from their long-range form.

Fig. 10 shows the experimental results of the Cahuzac and Toschek Eu–Sr experiment of [4]. The experiment again verifies the expected $R = \infty$ peak, and shows a characteristic skewing much like that of Fig. 7.

Discussion

An interesting feature of the dipole-dipole laser induced collision process is the occurrence of the peak cross section at the $R = \infty$ frequency of the separated atoms. From the quasi-molecular viewpoint of Fig. 3, one might at first expect the interaction to be strongest when the atoms are close together, and perhaps to have a linewidth which is much broader than that obtained theoretically or experimentally. The $R = \infty$ peak may be explained by noting that though the square of the dipole-dipole interaction energy varies as $1/R_x^6$, that this is offset by an increase of the square of the effective interaction time (13) as R_x^7. An additional R_x^2 dependence enters

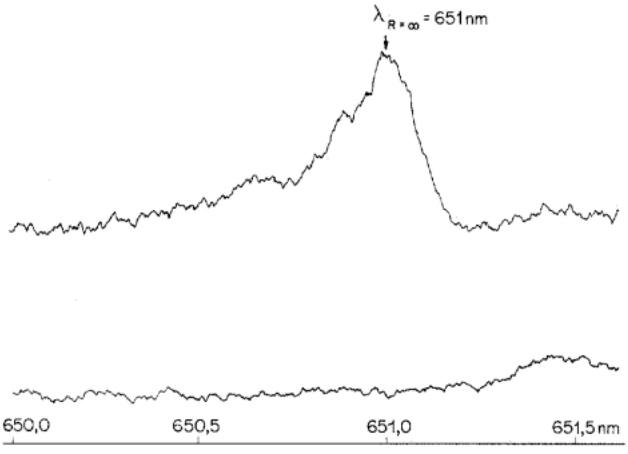

Fig. 10. Experimental lineshape of the Cahuzac and Toschek experiment of [4]. Energy was stored in the $6s6py\ ^8P_{7/2}$ level of Eu and transferred to the $5p^2\ ^1D_2$ level of Sr. Lower trace shows the noise level in the absence of the laser pump.

when integrating over impact parameter, leading to a net cross section which varies as R_x^3 in the wing (14). On this basis, we expect the $R = \infty$ peak to occur for dipole-dipole and dipole-quadrapole processes. For quadrapole-quadrapole, spin-exchange, charge-exchange, and free-bound processes, a peak at the $R = \infty$ frequency is not expected.

Finally, we note that the form of the lineshapes obtained here also applies to other types of dipole-dipole laser collisional processes. These include multiphoton processes, where several photons are absorbed before or after the virtual collision, Raman processes, and radiative collision lasers. In the latter case, lineshapes similar to those calculated should be observable via spontaneous emission.

Appendix
Evaluation of Orientationally Averaged Interaction Hamiltonian

We wish to find the orientationally averaged matrix elements of the dipole-dipole portion of the interaction Hamiltonian (2). We examine the case of s-p transitions, and assume that the initial orientation of the colliding atoms is random, and is maintained throughout the collision (the fixed atom approximation).

From the geometry of Fig. 2 we first have

$$\cos\theta = \frac{\rho}{R(t)} \tag{A1a}$$

$$\frac{dt}{R^3(t)} = \frac{\cos\theta}{\rho^2 V}\, d\theta \tag{A1b}$$

and

$$\int_{-\infty}^{+\infty} \frac{dt}{R^3(t)} = \int_{-\pi/2}^{\pi/2} \frac{\cos\theta}{\rho^2 V}\, d\theta = \frac{2}{\rho^2 V}. \tag{A1c}$$

We now assume that each of the three degenerate m states (of the p state atom) have equal probability of occupancy, separately compute their contribution to the cross section, and average the result. For the $m = 0$ state we have

$$\int_{-\infty}^{+\infty} \langle s \,|\, \mathcal{H}'(t) \,|\, p, m = 0\rangle dt = \int_{-\pi/2}^{\pi/2} \langle s \,|\, \frac{\cos\theta}{\rho^2 V} \cdot [x_A x_B (\sin\theta + \cos\theta)^2 + y_A y_B - 2 z_A z_B \cdot (\sin\theta - \cos\theta)^2] \,|\, p, m = 0\rangle \, d\theta = -\frac{4}{\rho^2 V} \mu^{A1} \mu^{B1} \tag{A2}$$

where μ^{A1} and μ^{B1} are the matrix elements, as seen by linearly polarized light of atoms A and B. Equation (A2) follows by substituting (2b) into (2a) and using $\langle s \,|\, x \,|\, p, m = 0\rangle = \langle s \,|\, y \,|\, p, m = 0\rangle = 0$, and $\langle s \,|\, z \,|\, p, m = 0\rangle = 1/\sqrt{3}$.

Proceeding as above, we also find

$$\int_{-\infty}^{+\infty} \langle s \,|\, \mathcal{H}'(t) \,|\, p, m = \pm 1\rangle dt = 0. \tag{A3}$$

We obtain the effective orientationally averaged interaction Hamiltonian by dividing each of the m state contributions by the trajectory integral [(A1c)], squaring each term, averaging the sum of squares, and taking the square root. The result is

$$\mathcal{H}'(t)_{\text{fixed atom}} = -\frac{2}{\sqrt{3}} \frac{\mu^{A1} \mu^{B1}}{R^3(t)}. \tag{A4}$$

Since the collision cross section is proportional to the square of the interaction Hamiltonian, we square before averaging.

We note that the assumption that the orientation of the atoms remains fixed during the collision is probably not correct at high field strengths. In the extreme of the rotating atom approximation, the effective interaction Hamiltonian is

$$\mathcal{H}'(t)_{\text{rotating atom}} = -\frac{2\mu^{A1} \mu^{B1}}{R^3(t)}. \tag{A5}$$

An exact treatment must explicitly retain the time dependence of the individual m states.

Acknowledgment

The authors wish to thank A. Gallagher and S. Payne for important early discussions and for preprints of their papers, and to Ph. Cahuzac and P. Toschek for allowing us to include their recent experimental results. They also wish to thank W. Green and J. Young for several discussions.

References

[1] L. I. Gudzenko and S. I. Yakovlenko, "Radiative collisions," *Sov. Phys. JETP*, vol. 35, pp. 877–881, 1972.

[2] S. E. Harris and D. B. Lidow, "Nonlinear optical processes by van der Waals interaction during collision," *Phys. Rev. Lett.*, vol. 33, pp. 674–676, 1974; —, *Phys. Rev. Lett.*, vol. 34, p. 172(E), 1975.

[3] S. E. Harris, R. W. Falcone, W. R. Green, D. B. Lidow, J. C. White, and J. F. Young, "Laser induced collisions," *Tunable Lasers and Applications*, A. Mooradian, T. Jaeger, and P. Stoketh, Eds. New York: Springer-Verlag, 1976, pp. 193–206; R. W. Falcone, W. R. Green, J. C. White, J. F. Young, and S. E. Harris, "Observation of laser-induced inelastic collisions," *Phys. Rev. A*, vol. 15, pp. 1333–1335, 1977; D. B. Lidow, R. W. Falcone, J. F. Young, and S. E. Harris, "Inelastic collision induced by intense optical radiation," *Phys. Rev. Lett.*, vol. 36, pp. 462–464, 1976; —, *Phys. Rev. Lett.*, vol. 37, p. 1590(E), 1976.

[4] Ph. Cahuzac and P. E. Toschek, "Light-assisted collisional energy transfer," *Laser Spectroscopy*, J. L. Hall and J. L. Carlsten, Eds. New York: Springer-Verlag, 1977.

[5] V. S. Lisitsa and S. I. Yakovlenko, "Optical and radiative collisions," *Sov. Phys. JETP*, vol. 39, pp. 759–763, 1974.

[6] A. Gallagher and T. Holstein, "Collision-induced absorption in atomic electronic transitions," to be published.

[7] M. G. Payne, C. W. Choi, and M. H. Nayfeh, "Laser induced collisional excitation transfer," presented at Int. Conf. Multiphoton Processes, Rochester, New York, June 6–9, 1977; M. G. Payne and M. H. Nayfeh, "Energy transfer between slowly moving atoms—The case of no crossing point," *Phys. Rev. A*, vol. 13, pp. 595–598, 1976.

[8] S. I. Yakovlenko, "Ionization of atoms in radiative collisions," *Sov. Phys. JETP*, vol. 37, pp. 1019–1022, 1973.

[9] L. I. Gudzenko and S. I. Yakovlenko, "Pair excitation of atoms in radiative collisions," *Phys. Lett.*, vol. 46A, pp. 475–476, 1974.

[10] S. Geltman, "Theory of laser-induced inelastic collisions," *J. Phys. B*, vol. 9, pp. L569–L574, 1976.

[11] —, "Laser-induced ionizing collisions in alkali vapors," to be published.

[12] T. F. George, J.-M. Yuan, I. H. Zimmerman, and J. R. Laing, "Radiative transitions for molecular collisions in an intense laser field," *Disc. Faraday Soc.*, no. 62, pp. 246–254, 1977; I. H. Zimmerman, J.-M. Yuan, and T. F. George, "Quantum mechanical theory of molecular collisions in a laser field," *J. Chem. Phys.*, vol. 66, pp. 2638–2646, 1977; J.-M. Yuan, J. R. Laing, and T. F. George, "Semiclassical theory of molecular collisions in a laser field," *J. Chem. Phys.*, vol. 66, pp. 1107–1121, 1977.

[13] N. M. Kroll and K. M. Watson, "Inelastic atom-atom scattering within an intense laser beam," *Phys. Rev. A*, vol. 13, pp. 1018–1033, 1976.

[14] A. M. F. Lau, "Nonperturbative theory of the resonant interaction of atoms with laser fields," *Phys. Rev. A*, vol. 14, pp. 279–290, 1976.

[15] D. A. Copeland and C. L. Tang, "On the optimal photon energy for photon-assisted nonresonant charge exchange," *J. Chem. Phys.*, vol. 66, pp. 5126–5129, 1977; —, "Photon-assisted nonresonant charge exchange: A simple molecular model," *J. Chem. Phys.*, vol. 65, pp. 3161–3171, 1976.

[16] P. L. Knight, "Laser-induced energy transfer and radiative collisions," *J. Phys. B*, vol. 10, pp. L195–L199, 1977.

[17] P. W. Milonni, "Laser-assisted excitation transfer as a single-atom multiphoton process," *J. Chem. Phys.*, vol. 66, pp. 3715–3719, 1977.

[18] J. L. Carlsten, A. Szoke, and M. G. Raymer, "Collisional redistribution and saturation of near-resonance scattered light," *Phys. Rev. A*, vol. 15, pp. 1029–1045, 1977.